

Improvement of cylindrical cloaking with the SHS lining

A. Greenleaf^{1,*}, Y. Kurylev², M. Lassas³ and G. Uhlmann⁴

¹*Department of Mathematics, University of Rochester, Rochester, NY 14627, USA*

²*Department of Mathematics, University College, London WC1E 6BT, UK*

³*Institute of Mathematics, Helsinki University of Technology, Espoo, FIN-02015, Finland*

⁴*Department of Mathematics, University of Washington, Seattle, WA 98195, USA*

* *Authors are in alphabetical order. Corresponding author: allan@math.rochester.edu*

Abstract: We analyze the effectiveness of cloaking an infinite cylinder from observations by electromagnetic waves in three dimensions. We show that, as truncated approximations of the ideal permittivity and permeability material parameters tend towards the singular ideal cloaking values, the D and B fields blow up near the cloaking surface. Since the metamaterials used to implement cloaking are based on effective medium theory, the resulting large variation in D and B poses a challenge to the suitability of the field-averaged characterization of ϵ and μ . We also consider cloaking with and without the SHS (soft-and-hard surface) lining. We demonstrate numerically that cloaking is significantly improved by the SHS lining, with both the far field of the scattered wave significantly reduced and the blow up of D and B prevented.

© 2007 Optical Society of America

OCIS codes: (160.1190) Materials: Anisotropic optical materials; (260.2110) Physical optics: Electromagnetic theory; (290.3200) Scattering: Inverse scattering

References and links

1. A. Greenleaf, M. Lassas and G. Uhlmann, "Anisotropic conductivities that cannot be detected in EIT," *Physiological Measurement (special issue on Impedance Tomography)*, **24**, 413–420 (2003).
2. A. Greenleaf, M. Lassas and G. Uhlmann, "On nonuniqueness for Calderón's inverse problem," *Math. Res. Lett.* **10**, 685–693 (2003).
3. U. Leonhardt, "Optical conformal mapping," *Science* **312**, 1777–1780 (23 June, 2006).
4. J.B. Pendry, D. Schurig and D.R. Smith, "Controlling electromagnetic fields," *Science* **312**, 1780–1782 (23 June, 2006).
5. J. B. Pendry, D. Schurig, D. R. Smith, "Calculation of material properties and ray tracing in transformation media," *Opt. Express* **14**, 9794 (2006).
6. A. Greenleaf, Y. Kurylev, M. Lassas and G. Uhlmann, "Full-wave invisibility of active devices at all frequencies," *ArXiv.org:math.AP/0611185v1,2,3* (2006); *Comm. Math. Phys.* **275**, 749–789 (2007).
7. S. Cummer, B.-I. Popa, D. Schurig, D. Smith and J. Pendry, "Full-wave simulations of electromagnetic cloaking structures," *Phys. Rev. E* 2006 Sep;74(3 Pt 2):036621.
8. D. Schurig, J. Mock, B. Justice, S. Cummer, J. Pendry, A. Starr and D. Smith, "Metamaterial electromagnetic cloak at microwave frequencies," *Science* **314**, 977–980 (10 Nov. 2006).
9. W. Cai, U. Chettiar, A. Kildishev and V. Shalaev, "Optical cloaking with metamaterials," *Nature Photonics*, **1**, 224–227 (April, 2007).
10. H. Chen and C. T. Chan, "Transformation media that rotate electromagnetic fields," *ArXiv.org:physics/0702050v1* (2007).
11. F. Zolla, S. Guenneau, A. Nicolet and J. Pendry, "Electromagnetic analysis of cylindrical invisibility cloaks and the mirage effect," *Opt. Lett.* **32**, 1069–1071 (2007).
12. G. Milton, M. Briane and J. Willis, "On cloaking for elasticity and physical equations with a transformation invariant form," *New J. Phys.* **8**, 248 (2006).

13. S. Cummer and D. Schurig, "One path to acoustic cloaking," *New Jour. Physics* **9**, 45 (2007).
14. G. Milton, "New metamaterials with macroscopic behavior outside that of continuum elastodynamics," ArXiv.org:070.2202v1 (2007).
15. S. Schelkunoff and H. Friis, *Antennas: Theory and Practice*, (Chapman and Hall, New York, 1952, 584–585).
16. A. Moroz, "Some negative refractive index material headlines...," <http://www.wave-scattering.com/negative.html>.
17. R. Weder, "A rigorous time-domain analysis of full-wave electromagnetic cloaking (Invisibility)," ArXiv.org:07040248v1,2,3 (2007).
18. A. Greenleaf, Y. Kurylev, M. Lassas and G. Uhlmann, "Electromagnetic wormholes and virtual magnetic monopoles from metamaterials," ArXiv.org:math-ph/0703059; *Phys. Rev. Lett.*, to appear.
19. A. Greenleaf, Y. Kurylev, M. Lassas and G. Uhlmann, "Electromagnetic wormholes via handlebody constructions," ArXiv.org:0704.0914v1, submitted (2007).
20. M. Yan, Z. Ruan, and M. Qiu, "Cylindrical invisibility cloak with simplified material parameters is inherently visible," ArXiv.org:0706.0655v1 (2007).
21. Z. Ruan, M. Yan, C. Neff and M. Qiu, "Confirmation of cylindrical perfect invisibility cloak using Fourier-Bessel analysis," ArXiv.org:0704.1183v1 (2007).
22. P.-S. Kildal, "Definition of artificially soft and hard surfaces for electromagnetic waves," *Electron. Lett.* **24**, 168–170 (1988).
23. P.-S. Kildal, "Artificially soft-and-hard surfaces in electromagnetics," *IEEE Trans Antennas Propag.*, **10**, 1537–1544 (1990).
24. I. Hänninen, I. Lindell, and A. Sihvola, "Realization of generalized Soft-and-Hard Boundary," *Progr. In Electromag. Res., PIER* **64**, 317–333 (2006).
25. I. M. Gel'fand and G. E. Shilov, *Generalized Functions, I-V* (Academic Press, New York, 1964).
26. A. Bossavit, A. *Computational electromagnetism. Variational formulations, complementarity, edge elements*, Academic Press Inc., San Diego, CA, 1998.
27. I. Lindell, *Differential Forms in Electromagnetics*, Wiley-IEEE Press, 2004.
28. C. Colton and R. Kress, *Inverse acoustic and electromagnetic scattering theory*. Second edition. Applied Math. Sciences, 93. (Springer-Verlag, Berlin, 1998).
29. M. Abramowitz and I. Stegun, *Handbook of mathematical functions with formulas, graphs, and mathematical tables* (U.S. Gov. Printing Office, Washington, D.C., 1964).
30. G. Milton, *The Theory of Composites* (Cambridge U. Press, 2001).
31. D. Smith and J. Pendry, "Homogenization of metamaterials by field averaging," *J. Opt. Soc. Am. B* **23**, 391–403 (2006).
32. R. Kohn, H. Shen, M. Vogelius and M. Weinstein, "Cloaking via change of variables in electric impedance tomography," preprint, <http://math.nyu.edu/faculty/kohn/papers/KSVW-cloaking.pdf> (2007).

1. Introduction

1.1. Background and history

There has recently been much activity concerning *cloaking*, or rendering objects invisible to detection by electromagnetic (EM) waves. For theoretical descriptions of EM material parameters of the general type considered here, see [1, 2, 3, 4, 5, 6]; for numerical and experimental results, see [7, 8, 9, 10, 11]. Related results concerning elastic waves are in [12, 13, 14]. All of these papers treat cloaking in the frequency domain, using time harmonic waves; this is not unreasonable, since the metamaterials used to implement these designs seem to be inherently prone to dispersion, for both practical and theoretical reasons [15, 16, 4]. See [17] for a treatment of cloaking in the time domain. One can also use similar ideas to design electromagnetic wormholes, which allow the passage of waves between possibly distant points while most of the wormhole remains invisible [18, 19].

When physically constructing a cloaking (or wormhole) device, one is of course not able to exactly match the ideal description of the EM material parameters (electric permittivity ϵ and magnetic permeability μ , for the purposes of this paper). Any actual implementation will only realize a discrete sampling of the values of ϵ and μ , and not be able to assume the ideal values at points x on the cloaking surface(s), where the tensors $\epsilon(x)$ or $\mu(x)$ have 0 or ∞ as eigenvalues.

1.2. Approximate cloaking and linings

The purpose of the current paper is twofold. First, we wish to explore the degradation of cloaking that occurs when the ideal material parameter fields are replaced with approximations obtained by limiting the *anisotropy ratio*, L , as described below. This was studied in two very interesting recent papers. Ruan, Yan, Neff and Qiu [21] consider the effect on cloaking of truncation of the the material parameter fields, while Yan, Ruan and Qiu [20], study the effect of using the simplified “reduced” material parameters employed in [8, 9]. In [21], it is shown that cloaking of passive objects, i.e., those with internal current $J = 0$, holds in the limit as $L \rightarrow \infty$, but a slow rate of convergence of the fields is noted. The current paper reproves this and demonstrates the blow up of the B and D fields at the cloaking surface as $L \rightarrow \infty$.

Secondly, we consider the effect of either including or not including a physical lining to implement the *soft-and-hard surface* (SHS) boundary condition, which is a boundary condition originally introduced in antenna design [22, 23, 24]. As we proved in [6], cloaking EM active objects, i.e., objects with generic internal current $J \neq 0$, imposes certain hidden boundary conditions on the waves propagating within the cloaked region. Any classical solution of Maxwell’s equations having locally finite energy, or even a weak solution of Maxwell’s equations with possible singularities, must satisfy these conditions. We note that in our terminology, the fields (E, H, D, B) are a finite energy solution if all the components $E_j, D_j, H_j,$ and B_j are locally integrable functions; the energy of the fields is locally finite; and they satisfy Maxwell’s equations in the classical or weak sense. The reason why we concentrate on such solutions is that the effective medium theory of metamaterial requires that the scale at which the EM fields change significantly is larger than the size of the components (or *cells*) used to implement the metamaterial; the blow up of the fields that is revealed by considering weak solutions presents a challenge to the effective material parameters described by such theories.

We consider a cylinder cloaked by what is called the *single coating* construction in [6], which corresponds to the cloaking considered in [1, 2, 4, 5]. (Note that the reduced parameters considered in [7, 8, 9, 20], while having similar geometry, have different material parameters and thus different waves.) For cylindrical cloaking, we showed in [6] that the hidden boundary conditions are the vanishing of the angular components of E and H . This is exactly the SHS condition associated with the angular vector field $\frac{\partial}{\partial \theta}$. We show that using a SHS lining has two benefits: blow up of B at the cloaking surface, which may seriously compromise effective medium theory for metamaterials, is prevented and secondly the farfield pattern of the scattered wave is greatly reduced. We remark that, although it was shown in [6] that there is no theoretical, frequency-dependent obstruction to cloaking, with current technology cloaking should nevertheless be considered as essentially monochromatic, and we will work at fixed frequency ω .

2. Single coating of a cylinder

Let us consider Maxwell’s equations on \mathbb{R}^3 ,

$$\begin{aligned}\nabla \times E &= i\omega B, \\ \nabla \times H &= -i\omega D, \\ D &= \varepsilon E, \\ B &= \mu H,\end{aligned}\tag{1}$$

where for simplicity we have taken the conductivity $\sigma = 0$. In empty space, $\varepsilon = \varepsilon_0$ and $\mu = \mu_0$ are isotropic and homogeneous. Throughout the paper we denote the wave number corresponding to the circular frequency ω by $k = \omega/c$, $c = 1/\sqrt{\varepsilon_0\mu_0}$.

We consider here EM waves propagating in metamaterials, which allow one to specify ϵ and μ fairly arbitrarily. Metamaterials are typically assembled from components whose size is somewhat smaller than the wavelength, λ . Ideal models of cloaking constructions consist of prescribed material parameters (tensor fields) ϵ, μ , describing coatings making objects invisible to detection by waves with frequency ω ; physically, these would be implemented using metamaterials designed to have ϵ, μ as effective parameters (at the specified frequency). Note that in the cloaking constructions the ideal parameters are singular on a surface surrounding the object, the *cloaking surface*, which we denote by Σ throughout. As a result, discussed further below, we need Maxwell's equations holding not only in the *classical* sense, i.e. for regular waves, but also in the sense of Schwartz distributions, i.e., for waves with singularities [25]. A distribution, or generalized function, u is a linear functional on a space of smooth test functions, f , generalizing the functional $u(f) := \int u(x)f(x)dx$ for locally integrable functions u . A solution to Maxwell's equations in the sense of distributions can be considered as a pair (E, H) which, when measured using a smooth superposition of point measurements, satisfy the same integral identities given by Green's theorem as do classical (smooth) solutions.

In the following, we describe the non-existence results for finite energy solutions with respect to the ideal parameter fields, the consequences of approximative material configurations, and the role of the SHS lining.

2.1. Equations for an ideal single coating

On \mathbb{R}^3 , with standard coordinates $x = (x_1, x_2, x_3)$, we use cylindrical coordinates (r, θ, z) , defined by $(r, \theta, z) \mapsto (r \cos \theta, r \sin \theta, z) \in \mathbb{R}^3$, so that $r = |(x_1, x_2)|$. In [6] we considered Maxwell's equations on $\mathbb{R}^3 \setminus \Sigma$,

$$\begin{aligned} \nabla \times \tilde{E} &= i\omega \tilde{B} \quad , \quad \nabla \times \tilde{H} = -i\omega \tilde{D} + \tilde{J}, \\ \tilde{D} &= \tilde{\epsilon} \tilde{E}, \quad \tilde{B} = \tilde{\mu} \tilde{H}, \end{aligned}$$

where $\tilde{\epsilon}$ and $\tilde{\mu}$ correspond to the invisibility coating materials on the exterior of the infinite cylinder $N_2 = \{r < 1\}$ and are homogeneous and isotropic inside N_2 , i.e., $\epsilon = \epsilon_0$ and $\mu = \mu_0$ in N_2 . Outside of N_2 , the material parameters $\tilde{\epsilon}$ and $\tilde{\mu}$ are matrix valued functions of x that are singular at the cloaking surface $\Sigma = \{r = 1\}$ that corresponds to the inner boundary of the metamaterial. As $r \rightarrow 1^+$,

$$\max_{1 \leq j, k \leq 3} \frac{\lambda_j(x)}{\lambda_k(x)} = O((r-1)^{-2}) \rightarrow \infty,$$

where $\lambda_j(x), j = 1, 2, 3$, are the eigenvalues of $\tilde{\epsilon}(x)$ or $\tilde{\mu}(x)$. In particular, we considered the question of when there are fields $\tilde{E}, \tilde{H}, \tilde{D}, \tilde{B}$ that together constitute a finite energy solution of Maxwell's equations. It was shown in [6] that, in the presence of generic internal currents \tilde{J} when the cloaked region is, e.g., a ball, such solutions do not generally exist. Let us discuss why this is so. Even for cloaking passive objects, i.e., $\tilde{J} = 0$ in the cloaked region, the singular material parameters give rise to solutions in Maxwell's equations that correspond either to surface currents (see below) or to the blow up in the fields at the cloaking surface. Thus, if the material does not allow such currents to appear, then the resulting fields must blow up.

Let us next consider the scattering of a plane wave by a cloaked cylinder, that is, the case when we have no internal currents and the EM fields have asymptotics at infinity corresponding to a sum of a given incident plane wave $(\tilde{E}^{in}, \tilde{H}^{in})$ and scattered wave $(\tilde{E}^{sc}, \tilde{H}^{sc})$ that satisfies the Silver-Müller radiation condition

$$\lim_{r \rightarrow \infty} r(\tilde{E}^{sc} \times e_r + \tilde{H}^{sc}) = 0, \quad (2)$$

where $e_r = x/|x|$ is the unit radial vector. It was shown in [6] that, with respect to cylindrical coordinates,

$$\lim_{r \rightarrow 1^+} e_\theta(x) \cdot \tilde{E}(x) = 0, \quad \lim_{r \rightarrow 1^+} e_\theta(x) \cdot \tilde{H}(x) = 0, \quad (3)$$

where e_θ is the angular unit vector (having Euclidian length = 1). Let e_z be the vertical unit vector. For general incoming waves, we have that

$$\begin{aligned} \lim_{r \rightarrow 1^+} e_z(x) \cdot \tilde{E}(x) - b_e \left(\frac{x}{|x|} \right) &= 0, \\ \lim_{r \rightarrow 1^+} e_z(x) \cdot \tilde{H}(x) - b_h \left(\frac{x}{|x|} \right) &= 0 \end{aligned} \quad (4)$$

where b_e and b_h do not vanish. In the treatment of cloaking passive objects [1, 2, 4, 5] it is assumed a priori, based on the behavior of rays on the exterior, that the inside of the cloaked region is “dark”, that is, the fields \tilde{E} and \tilde{H} vanish in $\{r < 1\}$. (However, see also [21, 20], where the behavior of the fields within the cloaked region is studied.) Under this assumption, the E and H fields have jumps across Σ ,

$$\begin{aligned} \left(\mathbf{v} \times \tilde{E} \right) |_{\Sigma^+} - \left(\mathbf{v} \times \tilde{E} \right) |_{\Sigma^-} &= \mathbf{v} \times \tilde{E} |_{\Sigma^+} = b_e(x) e_\theta, \\ \left(\mathbf{v} \times \tilde{H} \right) |_{\Sigma^+} - \left(\mathbf{v} \times \tilde{H} \right) |_{\Sigma^-} &= \mathbf{v} \times \tilde{H} |_{\Sigma^+} = b_h(x) e_\theta. \end{aligned}$$

(Here \mathbf{v} is the Euclidian normal vector of Σ , which is just the radial unit vector e_r .) This implies that Maxwell’s equations hold weakly on \mathbb{R}^3 :

$$\nabla \times \tilde{E} = i\omega \tilde{B} + \tilde{K}_{surf}, \quad \nabla \times \tilde{H} = -i\omega \tilde{D} + \tilde{J}_{surf}.$$

Here, δ_Σ is the Dirac delta distribution concentrated on Σ defined by

$$\delta_\Sigma(f) = \int_{\mathbb{R}^3} f(x) \delta_\Sigma dx := \int_\Sigma f(x) dS(x),$$

where $dS = d\theta dz$ is the Euclidian surface element on the surface Σ , for any smooth test function f . The singular terms $\tilde{K}_{surf} = b_e e_\theta \delta_\Sigma$, $\tilde{J}_{surf} = b_h e_\theta \delta_\Sigma$ can be considered either as magnetic and electric currents supported on Σ , or, as below, idealizing the blow up of \tilde{D} and \tilde{B} near Σ . We refer to such strongly singular field components as *surface currents*.

2.2. Equations for an approximate single coating.

Next, consider the situation when a metamaterial coating only approximates this ideal invisibility coating. We show that the existence of the surface currents for the ideal cloak causes a blow up of the fields as the approximating permittivity and permeability tend towards the singular ideal values, which we denote by $\tilde{\epsilon}$ and $\tilde{\mu}$.

To this end, we modify the construction described in the previous section, still dealing with a cloaking structure of the single coating type. More precisely, for $1 < R < 2$, consider an infinite cylinder in \mathbb{R}^3 given, in cylindrical coordinates, by $N_2^R = \{r < R\}$. On N_2^R we choose the metric to be Euclidian, so that the corresponding permittivity and permeability, ϵ_0 and μ_0 , are

homogeneous and isotropic. As described in §3, in $\mathbb{R}^3 \setminus N_2^R$, we take the Riemannian metric \tilde{g} and the corresponding permittivity and permeability $\tilde{\epsilon}$ and $\tilde{\mu}$ to be the single coating parameters considered in [6] and the previous section, truncated by being restricted to N_2^R . Thus, we start from the materials $\tilde{\epsilon}$ and $\tilde{\mu}$ corresponding to the single coating metric \tilde{g} outside N_2^R and replace the metric with the Euclidian metric inside N_2^R . Then the *anisotropy ratio*,

$$L_R := \sup_{x \in \mathbb{R}^3 \setminus N_2^R} \left(\max \frac{\lambda_j(x)}{\lambda_k(x)} \right) = O((R-1)^{-2}) \rightarrow \infty,$$

as the approximate cloaking construction approaches the ideal, that is, $R \rightarrow 1^+$.

Next, we consider the wave propagation phenomena that arise as the approximate cloaking construction approaches the ideal.

3. Analysis of solutions

Assume that the wave number $k = \omega/c$ is not a Neumann eigenvalue for the Euclidian Laplacian in the two-dimensional unit disk; as will be seen later, this is equivalent with the condition $(J_0)'(k) \neq 0$. For $1 < R < 2$ fixed, decompose \mathbb{R}^3 into

$$\begin{aligned} N_0 &= \{r \geq 2\}, \\ N_1^R &= \{R < r < 2\}, \text{ and} \\ N_2^R &= \{r \leq R\}. \end{aligned}$$

Let $\Sigma^R = \partial N_2^R = \{r = R\}$ be the (approximate) cloaking surface and $\nu = \partial_r$ be its normal vector on both sides, Σ_{R^\pm} . To define the approximate cloaking material parameters $\tilde{\epsilon}^R$ and $\tilde{\mu}^R$, define a relationship between material parameters ϵ, μ and a *Riemannian metric* g [1, 2, 6]. The permittivity and permeability, ϵ, μ corresponding to a metric $g = [g_{jk}(x)]_{j,k=1}^3$ are then given by

$$\epsilon^{jk} = \epsilon_0 |\det(g_{jk})|^{1/2} g^{jk}, \quad \mu^{jk} = \mu_0 |\det(g_{jk})|^{1/2} g^{jk}, \quad [g^{jk}] = [g_{jk}]^{-1}.$$

Define a set M^R consisting of three components,

$$\begin{aligned} M_0 &= \{r \geq 2\}, \\ M_1^R &= \{\rho < r < 2\}, \\ M_2^R &= \{r \leq R\}, \end{aligned}$$

where $\rho = 2(R-1)$. We identify the boundary of $M_0 \cup M_1^R$, i.e., the surface $\{(r, \theta, z) : r = \rho\}$, with the boundary of M_2^R , i.e., the surface $\{(r, \theta, z) : r = R\}$.

We equip M^R with the Euclidian metric g and the corresponding homogeneous, isotropic permittivity and permeability, $\epsilon = \epsilon_0, \mu = \mu_0$. With respect to the cylindrical coordinates, we have

$$g = [g_{jk}]_{j,k=1}^3 = \begin{pmatrix} 1 & 0 & 0 \\ 0 & r^2 & 0 \\ 0 & 0 & 1 \end{pmatrix}, \quad \epsilon = \epsilon_0 \begin{pmatrix} r & 0 & 0 \\ 0 & r^{-1} & 0 \\ 0 & 0 & r \end{pmatrix}, \quad \mu = \mu_0 \begin{pmatrix} r & 0 & 0 \\ 0 & r^{-1} & 0 \\ 0 & 0 & r \end{pmatrix}. \quad (5)$$

Next, introduce a transformation $F^R : M^R \rightarrow \mathbb{R}^3$, which in cylindrical coordinates is given by

$$\begin{aligned} F^R : M_0 &\rightarrow N_0, & F^R|_{M_0} &= id, \\ F^R : M_1^R &\rightarrow N_1^R, & F^R|_{M_1^R}(r, \theta, z) &= (r/2 + 1, \theta, z), \\ F^R : M_2^R &\rightarrow N_2^R, & F^R|_{M_2^R} &= id, \end{aligned}$$

see Fig. 1.

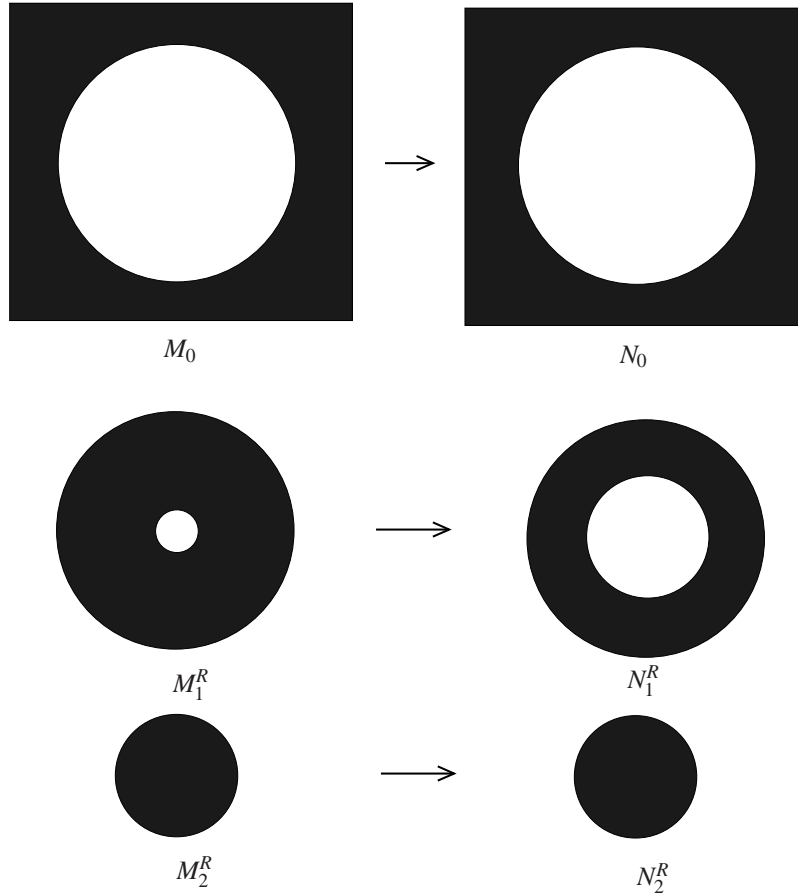


Fig. 1. Diagram of how the map F^R sends, in the plane $z = 0$, the components M_j^R of M^R to the components N_j^R of the approximate cloaking device N^R . Note that N^R is the union of $N_0 \cup N_1^R$ and N_2^R and thus is the space \mathbb{R}^3 , while M^R is a union of components $M_0 \cup M_1^R$ and M_2^R with boundaries identified and should not be thought of as lying in \mathbb{R}^3 .

We define the metric \tilde{g}^R on \mathbb{R}^3 by the formula $\tilde{g}^R = (F^R)^*g$, that is,

$$(\tilde{g}^R)^{jk}(y) = \sum_{p,q=1}^3 \frac{\partial y^j}{\partial x^p} \frac{\partial y^k}{\partial x^q} g^{pq}(x), \quad y = F^R(x),$$

where $[(\tilde{g}^{\kappa})^{J\kappa}] = [\tilde{g}_{jk}^{\kappa}]^{-1}$ and we use that $g^{pq} = \delta^{pq}$. Suppressing for the time being the superscript R , the permittivity and permeability, $\tilde{\epsilon}$, $\tilde{\mu}$ corresponding to the metric \tilde{g} are then given by $\tilde{\epsilon}^{jk} = \epsilon_0 |\det(\tilde{g}_{jk})|^{1/2} \tilde{g}^{jk}$ and $\tilde{\mu}^{jk} = \mu_0 |\det(\tilde{g}_{jk})|^{1/2} \tilde{g}^{jk}$. Here \tilde{g} , $\tilde{\epsilon}$, and $\tilde{\mu}$ are given by formula (5) on N_0 and N_2 , while on N_1 they are given by

$$\tilde{g} = \begin{pmatrix} 4 & 0 & 0 \\ 0 & 4(r-1)^2 & 0 \\ 0 & 0 & 1 \end{pmatrix},$$

$$\tilde{\epsilon} = \epsilon_0 \begin{pmatrix} (r-1) & 0 & 0 \\ 0 & (r-1)^{-1} & 0 \\ 0 & 0 & 4(r-1) \end{pmatrix}, \quad \tilde{\mu} = \mu_0 \begin{pmatrix} (r-1) & 0 & 0 \\ 0 & (r-1)^{-1} & 0 \\ 0 & 0 & 4(r-1) \end{pmatrix}.$$

In the following, we consider TE-polarized electromagnetic waves. This means that, written componentwise with respect to either coordinate system as

$$\tilde{E} = (\tilde{E}_1, \tilde{E}_2, \tilde{E}_3) = (\tilde{E}_r, \tilde{E}_\theta, \tilde{E}_z),$$

where the coordinates are such that if \tilde{E} is considered as a 1-form (see [26, 27]), then $\tilde{E} = \tilde{E}_1 dx^1 + \tilde{E}_2 dx^2 + \tilde{E}_3 dx^3$ is equal to $\tilde{E}_r dr + \tilde{E}_\theta d\theta + \tilde{E}_z dz$, that is,

$$\tilde{E}_r = \tilde{E}_1 \cos(\theta) + \tilde{E}_2 \sin(\theta), \quad \tilde{E}_\theta = r \left(-\tilde{E}_1 \sin(\theta) + \tilde{E}_2 \cos(\theta) \right), \quad \tilde{E}_z = \tilde{E}_3.$$

In the case of a TE-polarized wave the electric field has a nonzero component only in the z -direction,

$$\tilde{E}_1 = \tilde{E}_2 = \tilde{E}_r = \tilde{E}_\theta = 0, \quad \tilde{E}_3(x) = \tilde{E}_z(r, \theta).$$

We denote \tilde{E}_z by u , so that

$$\tilde{H} = \frac{1}{i\omega} \tilde{\mu}^{-1} (\nabla \times \tilde{E}) = \frac{1}{i\omega} \tilde{\mu}^{-1} (\nabla u \times e_z).$$

We note that u satisfies the (scalar) Helmholtz equation,

$$(\Delta_{\tilde{g}} + k^2)u = 0 \quad \text{on } \mathbb{R}^3$$

where $\Delta_{\tilde{g}}$ is the Laplace-Beltrami operator [1, 6] corresponding to the metric \tilde{g} and $k = \omega \sqrt{\epsilon_0 \mu_0}$. Recall for the following that $k = \omega/c$, $c = 1/\sqrt{\epsilon_0 \mu_0}$.

3.1. Scattering problem

We consider an incoming TE polarized plane wave. In N_0 such a wave has the form

$$\tilde{E}_{in}(r, \theta, z) = A e^{ikr \cos \theta} e_z = A \left(J_0(kr) + \sum_{n=1}^{\infty} 2i^n J_n(kr) \cos(n\theta) \right) e_z,$$

$$\tilde{H}_{in}(r, \theta, z) = \frac{c}{ik} \mu_0^{-1} \nabla \times \tilde{E}_{in},$$

where A is a constant; expressed in terms of $\tilde{u}_{in} = E_{3,in}$, this is

$$\tilde{u}_{in} = A(J_0(kr) + \sum_{n=1}^{\infty} 2i^n J_n(kr) \cos(n\theta)).$$

We look for the solution of the scattering problem,

$$\begin{aligned} \nabla \times \tilde{E} &= i\omega\tilde{B}, & \nabla \times \tilde{H} &= -i\omega\tilde{D}, \\ \tilde{D} &= \tilde{\epsilon}\tilde{E}, & \tilde{B} &= \tilde{\mu}\tilde{H} \end{aligned} \quad (6)$$

on \mathbb{R}^3 , where $\tilde{\epsilon} = \tilde{\epsilon}^R$, $\tilde{\mu} = \tilde{\mu}^R$ so that $\tilde{E} = \tilde{E}^R$, etc. Suppressing again the index R , $\tilde{E} = \tilde{E}_{in} + \tilde{E}_{sc}$, $\tilde{H} = \tilde{H}_{in} + \tilde{H}_{sc}$, and \tilde{E}_{sc} and \tilde{H}_{sc} satisfy the Silver-Müller radiation condition (2). (Cylindrical cloaking is also studied using Fourier-Bessel series in [21].)

We now analyze the waves in the three components of \mathbb{R}^3 , N_0, N_1, N_2 . In the domain $N_0 = \{r \geq 2\}$, one has

$$\begin{aligned} \tilde{E}_{sc}(r, \theta, z) &= \left(\sum_{n=0}^{\infty} c_n H_n^{(1)}(kr) \cos(n\theta) \right) e_z, \\ \tilde{H}_{sc}(r, \theta, z) &= \frac{c}{ik} \mu_0^{-1} (\nabla \times \tilde{E}_{sc}), \\ \tilde{u}_{sc} &= \sum_{n=0}^{\infty} c_n H_n^{(1)}(kr) \cos(n\theta). \end{aligned}$$

Now use the change of coordinates, $F : M \rightarrow N$ to define the transformed fields on M ,

$$\begin{aligned} E_{in} &= F^* \tilde{E}_{in}, & H_{in} &= F^* \tilde{H}_{in}, \\ E_{sc} &= F^* \tilde{E}_{sc}, & H_{sc} &= F^* \tilde{H}_{sc}, \\ E &= F^* \tilde{E}, & H &= F^* \tilde{H}. \end{aligned}$$

In the coordinates $(r', \theta', z') = F^{-1}(r, \theta, z)$, $\theta' = \theta, z' = z$ on $M_0 = F^{-1}(N_0)$,

$$\begin{aligned} \nabla \times E &= i\omega B, & \nabla \times H &= -i\omega D, \\ D &= \epsilon_0 E, & B &= \mu_0 H. \end{aligned}$$

In M_1 , i.e., for $r' > \rho$,

$$\begin{aligned} E(r', \theta', z') &= \left(A J_0(kr') + c_0 H_0^{(1)}(kr') + \sum_{n=1}^{\infty} (2i^n A J_n(kr') + c_n H_n^{(1)}(kr')) \cos(n\theta') \right) e_z, \\ H(r', \theta', z') &= \frac{c}{ik} \mu_0^{-1} (\nabla \times E), \\ u(r', \theta') &= E_3(r', \theta') = A J_0(kr') + c_0 H_0^{(1)}(kr') + \\ &\quad + \sum_{n=1}^{\infty} (2i^n A J_n(kr') + c_n H_n^{(1)}(kr')) \cos(n\theta'). \end{aligned}$$

In N_1 , where $R < r < 2$, we have generally

$$\begin{aligned}\tilde{E}_r(r, \theta, z) &= 2E_r(2(r-1), \theta, z), & \tilde{E}_\theta(r, \theta, z) &= E_\theta(2(r-1), \theta, z), \\ \tilde{E}_z(r, \theta, z) &= E_z(2(r-1), \theta, z).\end{aligned}$$

In the case of TE-polarized field E_r and E_θ vanish. In N_2 , i.e., for $r \leq R$,

$$\begin{aligned}\tilde{E}(r, \theta, z) &= \left(\sum_{n=0}^{\infty} a_n J_n(kr) \cos(n\theta) \right) e_z, \\ \tilde{u}(r, \theta) &= \sum_{n=0}^{\infty} a_n J_n(kr) \cos(n\theta), \\ \tilde{H}(r, \theta, z) &= \frac{c}{ik} \mu_0^{-1} (\nabla \times \tilde{E}).\end{aligned}\tag{7}$$

As $F|_{M_2^R} = id$, the fields E and H and the potential u are also given by (7) in M_2 .

On $\Sigma^R = \partial N_2^R$, using the standard transmission conditions for the electric and magnetic fields, which ensure that waves are at least weak solutions of Maxwell's equations, are

$$\begin{aligned}\tilde{E}_\theta|_{\Sigma_{R^+}} &= \tilde{E}_\theta|_{\Sigma_{R^-}}, & \tilde{E}_z|_{\Sigma_{R^+}} &= \tilde{E}_z|_{\Sigma_{R^-}}; \\ \tilde{H}_\theta|_{\Sigma_{R^+}} &= \tilde{H}_\theta|_{\Sigma_{R^-}}, & \tilde{H}_z|_{\Sigma_{R^+}} &= \tilde{H}_z|_{\Sigma_{R^-}}; \\ \tilde{D}_r|_{\Sigma_{R^+}} &= \tilde{D}_r|_{\Sigma_{R^-}}; & \tilde{B}_r|_{\Sigma_{R^+}} &= \tilde{B}_r|_{\Sigma_{R^-}},\end{aligned}$$

from which we get the following transmission conditions for \tilde{u} :

$$\begin{aligned}\tilde{u}|_{\Sigma_{R^+}} &= \tilde{u}|_{\Sigma_{R^-}}, \\ (R-1) \partial_r \tilde{u}|_{\Sigma_{R^+}} &= R \partial_r \tilde{u}|_{\Sigma_{R^-}}.\end{aligned}$$

These correspond to conditions on $\partial M_2^R = \partial(M_0^R \cup M_1^R)$,

$$\begin{aligned}u^+|_{r=\rho^+}(\theta, z) &= u^-|_{r=R^-}(\theta, z), \\ \rho \partial_r u^+|_{r=\rho^+}(\theta, z) &= R \partial_r u^-|_{r=R^-}(\theta, z),\end{aligned}$$

where $u^+ = u|_{M_1^R}$ and $u^- = u|_{M_2^R}$.

These conditions give rise to equations for c_n and a_n ; let us start with $n = 0$, which is of particular interest. We have

$$\begin{aligned}a_0 J_0(kR) &= A J_0(k\rho) + c_0 H_0^{(1)}(k\rho), \\ a_0 R k (J_0)'(kR) &= A \rho k (J_0)'(k\rho) + c_0 \rho k (H_0^{(1)})'(k\rho)\end{aligned}$$

Now explicitly denoting the dependence of a_n and c_n on R , we see that, when $(J_0)'(k) \neq 0$, these imply that

$$\begin{aligned}c_0(R) &= A \frac{\rho (J_0)'(k\rho) J_0(kR) - R J_0(k\rho) (J_0)'(kR)}{\rho (H_0^{(1)})'(k\rho) J_0(kR) - R H_0^{(1)}(k\rho) (J_0)'(kR)} = iA\pi \frac{1}{\log(k\rho)} (1 + o(1)), \\ a_0(R) &= A \frac{\rho J_0(k\rho) (H_0^{(1)})'(k\rho) - \rho (J_0)'(k\rho) H_0^{(1)}(k\rho)}{\rho (H_0^{(1)})'(k\rho) J_0(kR) - R H_0^{(1)}(k\rho) (J_0)'(kR)} = \frac{-2A\pi}{(J_0)'(k) \log(k\rho)} (1 + o(1)),\end{aligned}$$

where we use the asymptotics of Bessel functions near 0, see [29, pp.360–1]. Here, $o(1)$ means that the quantity goes to zero as $R \rightarrow 1^+$, $\rho \rightarrow 0^+$. Similarly, a_n and c_n satisfy the equations,

$$\begin{aligned} a_n J_n(kR) &= A J_n(k\rho) + c_n H_n^{(1)}(k\rho), \\ a_n R k (J_n)'(kR) &= A \rho k (J_n)'(k\rho) + c_n \rho k (H_n^{(1)})'(k\rho). \end{aligned}$$

For generic k , these yield that

$$\begin{aligned} c_n(R) &= A \frac{\rho (J_n)'(k\rho) J_n(kR) - R J_n(k\rho) (J_n)'(kR)}{\rho (H_n^{(1)})'(k\rho) J_n(kR) - R H_n^{(1)}(k\rho) (J_n)'(kR)} = O(\rho^{2n}), \\ a_n(R) &= A \frac{\rho J_n(k\rho) (H_n^{(1)})'(k\rho) - \rho (J_n)'(k\rho) H_n^{(1)}(k\rho)}{\rho (H_n^{(1)})'(k\rho) J_n(kR) - R H_n^{(1)}(k\rho) (J_n)'(kR)} = O(\rho^n). \end{aligned} \quad (8)$$

This implies that the scattered fields (far field patterns) $\tilde{E}_{sc}, \tilde{H}_{sc}$ in $N_0 \cup N_1^R$ and the transmitted fields \tilde{E}, \tilde{H} in N_2^R , which, as we recall, depend on R , go to zero as the approximate cloaking construction tends to the ideal material parameters, i.e., $R \rightarrow 1^+$. A similar result was obtained in [21].

Next, we consider the behavior of the fields $\tilde{E}^R, \tilde{H}^R, \tilde{D}^R, \tilde{B}^R$ near Σ^R . Suppressing again the superscript R , we write the electric and magnetic fields as

$$\begin{aligned} \tilde{E}(r, \theta, z) &= \sum_{n=0}^{\infty} \tilde{E}^n(r, \theta, z), \quad \text{where} \quad \tilde{E}^n(r, \theta, z) = f_n(kr) \cos(n\theta) e_z; \\ \tilde{H}(r, \theta, z) &= \sum_{n=0}^{\infty} \tilde{H}^n(r, \theta, z), \quad \text{where} \quad \tilde{H}^n(r, \theta, z) = \frac{c}{ik} \tilde{\mu}^{-1} \left(\nabla \times \tilde{E}^n(r, \theta, z) \right), \end{aligned} \quad (9)$$

with similar notations for the scattered and incoming fields, $\tilde{E}_{sc}^n, \tilde{H}_{sc}^n$, etc. On M , the decomposition (9) gives rise to a similar decomposition of E and H , which we analyze for each value of n . First, we consider the terms corresponding to $n = 0$. On $M_0 \cup M_1^R$, at $y = F_1^{-1}(x), y = (r', \theta', z'), x \in N_0 \cup N_1^R$,

$$\begin{aligned} E_{in,z}^0(y) &= A J_0(kr') = O(1), \\ E_{sc,z}^0(y) &= c_0(R) H_0^{(1)}(kr') = -A \frac{\ln(kr')}{\ln(k\rho)} (1 + o(1)) \end{aligned}$$

as $R \rightarrow 1^+$. Observe that, since $r' \geq \rho$, $E_{sc,z}^0(y)$ is uniformly bounded for $R \rightarrow 1^+$. With the magnetic field, expressed as $H^0 = H_r^0 dr + H_\theta^0 d\theta + H_z^0 dz$, having a non-zero component only in θ , one has

$$\begin{aligned} H_{in,\theta}^0(y) &= \frac{iAc}{\mu_0} r' (J_0)'(kr') = O((r')^2); \\ H_{sc,\theta}^0(y) &= \frac{iAc}{\mu_0} r' c_0(R) \left(H_0^{(1)} \right)'(kr') = \frac{iAc}{\mu_0 k \ln(k\rho)} (1 + o(1)). \end{aligned}$$

On M_2^R ,

$$E_z^0(y) = a_0(R)J_0(kr') = \frac{O(1)}{\ln(k\rho)};$$

$$H_\theta^0(y) = \frac{c}{\mu_0}ia_0(R)r'(J_0)'(kr') = \frac{O(1)}{\ln(k\rho)}.$$

Returning to N and again using the transformation rules for E and H , we see that \tilde{E}^0, \tilde{H}^0 are uniformly bounded, with respect to R , in $N_1^R \cup N_2^R$.

Now consider the magnetic flux density, $\tilde{B} = \tilde{\mu}\tilde{H}$ which has a similar decomposition. In particular, on N_1^R , one has

$$\tilde{B}_{in,\theta}^0(r, \theta) = \tilde{\mu}\tilde{H}_{in,\theta}^0(r, \theta) = \tilde{\mu}H_{in,\theta}^0(2(r-1), \theta) = O(r-1), \quad (10)$$

$$\tilde{B}_{sc,\theta}^0(r, \theta) = \tilde{\mu}\tilde{H}_{sc,\theta}^0(r, \theta) = \tilde{\mu}H_{sc,\theta}^0(2(r-1), \theta) = \frac{Aci}{k(r-1)\ln(k\rho)}(1+o(1)).$$

Pointwise, on N_2^R ,

$$\tilde{B}_\theta^0(r, \theta) = \frac{O(r)}{\ln(k\rho)},$$

tending to 0 when $R \rightarrow 1^+$ for all points outside Σ . To see how \tilde{B}_θ^0 behaves near Σ when $R \rightarrow 1^+$, observe that (10) implies that $\int_{1/2}^{3/2} \tilde{B}_\theta^0(r, \theta) dr$ is uniformly bounded, while, for any $0 < \kappa < \frac{1}{2}$,

$$\int_{1-\kappa}^{1+\kappa} \tilde{B}_\theta^0(r, \theta) dr = \frac{Aci}{k} \int_{\rho/2}^{\kappa} \frac{1}{(\log \rho)t} dt + o(1) \rightarrow \frac{Aci}{k} \quad \text{when } R = \rho/2 + 1 \rightarrow 1^+.$$

This implies that

$$\lim_{R \rightarrow 1^+} \tilde{B}_\theta^0 = \frac{Aci}{k} \delta_\Sigma + \tilde{B}_{b,\theta}^0,$$

where δ_Σ is the Dirac delta function of the cylinder $\Sigma = \{r = 1\}$ and $\tilde{B}_{b,\theta}^0$ is a bounded function.

Finally, consider \tilde{D}^0 which has only the z -component different from 0. In N_1^R ,

$$\tilde{D}_{in,z}^0(r, \theta) = \tilde{\epsilon}\tilde{E}_{in,z}^0(r, \theta) = \epsilon_0(r-1)E_{in,z}^0(2(r-1), \theta) = O(r-1);$$

$$\tilde{D}_{sc,z}^0(r, \theta) = \tilde{\epsilon}\tilde{E}_{sc,z}^0(r, \theta) = \epsilon_0(r-1)E_{sc,z}^0(2(r-1), \theta) = \frac{O((r-1)\ln(r-1))}{\ln(k\rho)},$$

while in N_2^R ,

$$\tilde{D}_z^0(r, \theta) = \tilde{\epsilon}\tilde{E}_z^0(r, \theta) = \epsilon_0 E_z^0(r, \theta) = \frac{O(1)}{\ln(k\rho)}.$$

Thus, when $R \rightarrow 1^+$, $\tilde{D}_{in,z}^0$ has a uniform limit in $N_0 \cup N_1$, and $\tilde{D}_{sc,z}^0, \tilde{D}_z^0$ uniformly tend to 0 in $N_0 \cup N_1, N_2$, respectively.

For $n \geq 1$, using (8), we obtain the following asymptotics for E , etc., in the various components of N :

In N_1^R , where $r > R$, i.e. $2(r' - 1) > \rho$,

$$\begin{aligned}\tilde{E}_{in,z}^n &= O((r-1)^n), & \tilde{E}_{sc,z}^n &= O\left(\frac{\rho^{2n}}{(r-1)^n}\right); \\ \tilde{H}_{in,r}^n &= O((r-1)^{n-1}), & \tilde{H}_{sc,r}^n &= O\left(\frac{\rho^{2n}}{(r-1)^{n+1}}\right), \\ \tilde{H}_{in,\theta}^n &= O((r-1)^n), & \tilde{H}_{sc,\theta}^n &= O\left(\frac{\rho^{2n}}{(r-1)^n}\right); \\ \tilde{D}_{in,z}^n &= O((r-1)^{n+1}), & \tilde{D}_{sc,z}^n &= O\left(\frac{\rho^{2n}}{(r-1)^{n-1}}\right); \\ \tilde{B}_{in,r}^n &= O((r-1)^n), & \tilde{B}_{sc,r}^n &= O\left(\frac{\rho^{2n}}{(r-1)^n}\right), \\ \tilde{B}_{in,\theta}^n &= O((r-1)^{n-1}), & \tilde{B}_{sc,\theta}^n &= O\left(\frac{\rho^{2n}}{(r-1)^{n+1}}\right).\end{aligned}$$

As for N_2^R , we have

$$\begin{aligned}\tilde{E}_z^n &= O(\rho^n); & \tilde{D}_z^n &= O(\rho^n); \\ \tilde{H}_r^n &= O(\rho^n), & \tilde{H}_\theta^n &= O(\rho^n); \\ \tilde{B}_r^n &= O(\rho^n), & \tilde{B}_\theta^n &= O(\rho^n).\end{aligned}$$

These formulae imply that there is a uniform limit of $\tilde{E}^n, \tilde{H}^n, \tilde{D}^n, \tilde{B}^n$ when $R \rightarrow 1^+$ and, moreover, the scattered fields in $N_0 \cup N_1$ and transmitted fields in N_2 tend to 0. These formulae also imply that the series

$$\sum_{n=1}^{\infty} \tilde{E}_{sc}^n, \quad \sum_{n=1}^{\infty} \tilde{H}_{sc}^n, \quad \sum_{n=1}^{\infty} \tilde{B}_{sc}^n, \quad \sum_{n=1}^{\infty} \tilde{D}_{sc}^n,$$

in $N_0 \cup N_1$; and

$$\sum_{n=1}^{\infty} \tilde{E}^n, \quad \sum_{n=1}^{\infty} \tilde{H}^n, \quad \sum_{n=1}^{\infty} \tilde{B}^n, \quad \sum_{n=1}^{\infty} \tilde{D}^n,$$

all converge to zero in N_2 as $R \rightarrow 1^+$.

Summarizing, we see that, in the sense of distributions,

$$\begin{aligned}\lim_{R \rightarrow 1^+} \tilde{E}^R &= \tilde{E}_b, & \lim_{R \rightarrow 1^+} \tilde{H}^R &= \tilde{H}_b, \\ \lim_{R \rightarrow 1^+} \tilde{D}^R &= \tilde{D}_b - \frac{1}{i\omega} \tilde{J}_{surf}, & \tilde{J}_{surf} &= 0, \\ \lim_{R \rightarrow 1^+} \tilde{B}^R &= \tilde{B}_b + \frac{1}{i\omega} \tilde{K}_{surf}, & \tilde{K}_{surf} &= -Ae_\theta \delta_\Sigma.\end{aligned}$$

Here $E_b, H_b, D_b,$ and B_b coincide with $E_{in}, H_{in}, B_{in},$ and $B_{in},$ resp., in $N_0 \cup N_1$ and are equal to 0 in N_2 . In particular, they satisfy equations (6) separately in $N_0 \cup N_1$ and N_2 .

Note that, sending an TM-polarized wave, we get that $\tilde{J}_{surf} = -Ae_\theta \delta_\Sigma, \tilde{K}_{surf} = 0$. Moreover, for a general incoming electromagnetic wave, the corresponding solutions $\tilde{E}^R, \tilde{H}^R, \tilde{D}^R, \tilde{B}^R$ tend to $\tilde{E}_{lim}, \tilde{H}_{lim}, \tilde{D}_{lim}, \tilde{B}_{lim},$ which satisfy

$$\begin{aligned} \nabla \times \tilde{E}_{lim} &= i\omega \tilde{B}_{lim} + \tilde{K}_{surf}, & \nabla \times \tilde{H}_{lim} &= -i\omega \tilde{D}_{lim} + \tilde{J}_{surf}, \\ \tilde{D}_{lim} &= \tilde{\epsilon} \tilde{E}_{lim}, & \tilde{B}_{lim} &= \tilde{\mu} \tilde{H}_{lim}, \end{aligned}$$

with $\tilde{J}_{surf} = b_e e_\theta \delta_\Sigma, \tilde{K}_{surf} = b_h e_\theta \delta_\Sigma$.

4. Numerical results

We next use the analytic expressions found above to compute the fields for a plane wave with vertically polarized E-field, $E_{in}(r, \theta, z) = A e^{ikr \cos \theta} e_z$. The computations are made without reference to physical units; for simplicity, we use $\mu_0 = 1, \epsilon_0 = 1,$ amplitude $A = 1$ and wavenumber $k = 3$. The wave E_{in} is incident to a cylinder $\{r < R\}$ that is coated with an approximative invisibility cloaking layer located in $\{R < r < 2\}$. We then numerically simulate the cases where $R = 1.01$ and $R = 1.05$. In the simulations we have used Fourier series representation to order 6, that is, the fields are represented using trigonometric polynomials of degree less than or equal to six, $\sum_{|n| \leq 6} f_n(r) e^{in\theta}$. In the tables below, we give the real parts of the y-component of the total fields and the scattered B-field on the line $\{(x, 0, 0) : x \in [0, 3]\}$, first in the absence of a physical layer inside the metamaterial and then when an SHS lining is included. We note that in the case of the SHS lining, the fields are as was claimed in [4, 7, 8, 17] without reference to a lining, namely zero inside the cylinder $\{r < R\}$.

Below we give the numerically computed Fourier coefficients of the scattered waves. The values for $R = 1.05$, for which $L_R = 1600$, and $R = 1.01$, for which $L_R = 40,000$, are contained in the following two tables.

Table 1. Fourier coefficients of scattered waves for $R = 1.05$

n	c_n with SHS lining	c_n with no SHS lining
0	$-0.0042 - 0.0644i$	$-0.7408 - 0.4382i$
1	$-0.1407 - 0.0099i$	$0.0838 - 0.0035i$
2	$0.0000 - 0.0016i$	$0.0000 - 0.0013i$
3	$0.0000 + 0.0000i$	$0.0000 + 0.0000i$
4	$0.0000 + 0.0000i$	$0.0000 + 0.0000i$
5	$0.0000 + 0.0000i$	$0.0000 + 0.0000i$
6	$0.0000 + 0.0000i$	$0.0000 + 0.0000i$
$(\sum c_n ^2)^{1/2}$	0.1551	0.8648

Table 2. Fourier coefficients of scattered waves for $R = 1.01$

n	c_n with SHS lining	c_n with no SHS lining
0	$-0.0000 - 0.0028i$	$-0.2591 - 0.4382i$
1	$-0.0057 - 0.0000i$	$0.0031 - 0.0000i$
2	$0.0000 + 0.0000i$	$0.0000 + 0.0000i$
3	$0.0000 + 0.0000i$	$0.0000 + 0.0000i$
4	$0.0000 + 0.0000i$	$0.0000 + 0.0000i$
5	$0.0000 + 0.0000i$	$0.0000 + 0.0000i$
6	$0.0000 + 0.0000i$	$0.0000 + 0.0000i$
	$(\sum c_n ^2)^{1/2}$	
	0.0063	0.5091

The results show that for R close to 1, including the SHS lining strongly reduces the far field of the scattered wave; the approximative invisibility cloaking functions much better with such a lining than without, even for cloaking passive objects.

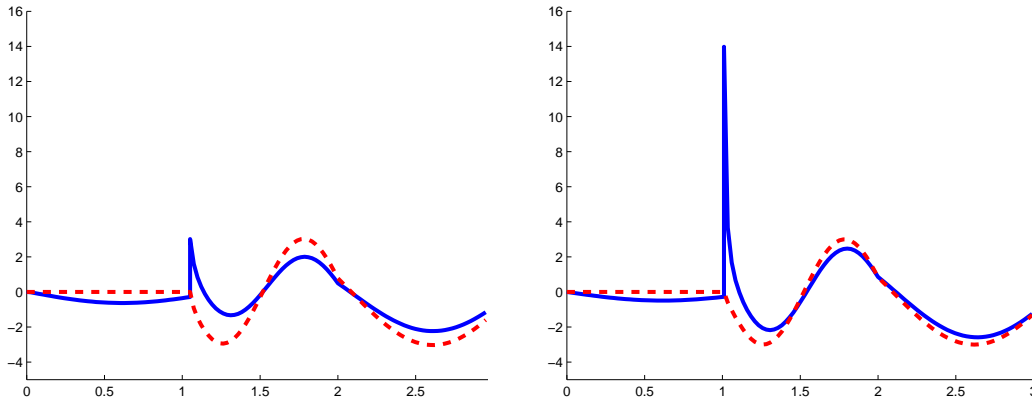


Fig. 2. The real part of the y -component of the **total** B -field on the line $\{(x, 0, 0) : x \in [0, 3]\}$. Blue solid curve is the field with no physical lining at $\{r = R\}$. Red dashed curve is the field with SHS lining on $\{r = R\}$. In the left figure, $R = 1.05$ and the maximal anisotropy ratio is $L_R = 1600$. In the right figure, $R = 1.01$ and the maximal anisotropy ratio is $L_R = 40,000$.

In Fig. 2, we see clearly that the *total* field develops a delta-type distributional singularity on the interface when we do not have the SHS lining and the approximative cloaking approaches the ideal, i.e., $R \rightarrow 1^+$. Also, in Fig. 3, we see that, far away from the coated cylinder, in both cases the *scattered* field goes to zero, but much more quickly when the SHS lining is used.

5. Discussion

5.1. Comparison of results with and without SHS.

One observes that, without the SHS lining, the B -field grows as the approximate single coating tends to the ideal invisibility cloak, i.e., as the anisotropy ratio L_R becomes larger. In both parts of Fig. 2, the peak near $r = 1$ without the SHS lining illustrates how the delta-distribution in the B -field develops.

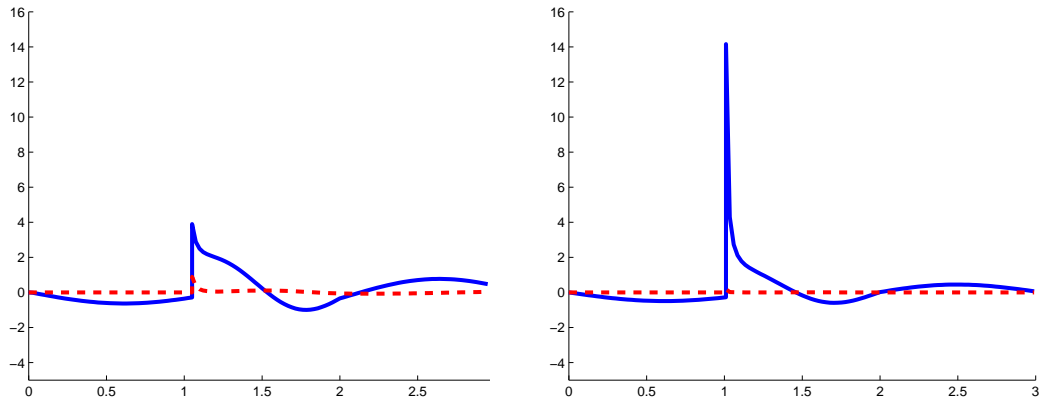


Fig. 3. The real part of the y -component of the **scattered** B -field on the line $\{(x, 0, 0) : x \in [0, 3]\}$. Blue solid curve is the field with no physical lining at $\{r = R\}$. Red dashed line is the field with Soft-and-Hard lining on $\{r = R\}$. In the left figure, $R = 1.05$ and the maximal anisotropy ratio is $L_R = 1600$. In the right figure, $R = 1.01$ and the maximal anisotropy ratio is $L_R = 40,000$.

Note that the value of the anisotropy ratio L_R is quite large in our simulation, but the resulting fields are still not extremely large. The blow up of the fields when an SHS lining is not used seems likely to become more significant as cloaking technology develops. The SHS boundary lining has the additional benefit in our simulations of making the scattered wave smaller outside of the metamaterial construction. Indeed, the scattered field when using the SHS boundary lining is less than 2% of the scattered field without the lining. The reduction in the scattered field with the SHS lining is further illustrated in Figs. 4 and 5.

Thus, implementation of a lining significantly improves the cloaking effect.

5.2. Significance of the surface currents \tilde{J}_{surf} and \tilde{K}_{surf}

For generic incoming waves, as $R \rightarrow 1^+$ the magnetic and electric flux densities converge to fields that contain delta-function type components supported on the surface Σ . We phrase this by saying that *surface currents* appear. If the metamaterial in question supports such currents, then we interpret this literally. This holds, e.g., if the metamaterials used have components near Σ that approximate a SHS surface, such as strips of PEC and PMC materials. Alternatively, if such highly localized currents can not be carried by the material, then \tilde{D} and \tilde{B} will blow up as the approximation of the coating material goes to the ideal limit, $R \rightarrow 1^+$.

Effective medium theory for composite materials is proven only when the limiting fields are relatively smooth [30]. Such rigorous effective medium theory has not yet been established for metamaterials, but the limited work so far, e.g., [31], clearly indicate that this same restriction will hold there as well. One can then interpret the blow up of fields as a challenge to the validity of the material parameters that have been ascribed to the metamaterials currently employed. Indeed, fields having a blow up are very rapidly changing functions near the cloaking surface Σ . Thus, a physical cloaking construction that would operate well with such fields would require metamaterials whose cell size becomes very small close to the cloaking surface. The simplest way to avoid these issues might be to include the SHS lining when constructing the cloaking

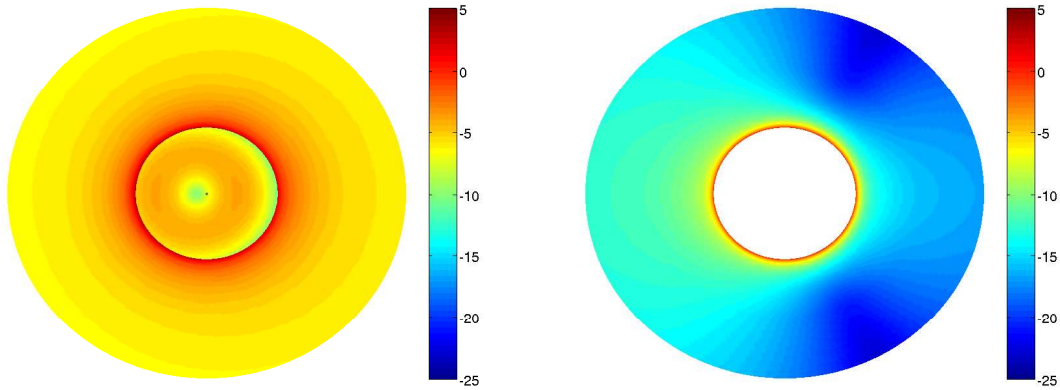


Fig. 4. **The magnitudes of the scattered B -fields on the exterior for $L_R = 1600$.** The decibel function $10 \times \log_{10}(|B_{sc}|/|B_{in}|)$ is shown on a color scale. The left figure corresponds to the field in the absence of an SHS lining, while the right figure corresponds to the field with the SHS lining.

device.

5.3. Summary

We have considered two cases when cloaking an infinite cylinder:

(1) An infinite cylinder of air or vacuum, is coated with metamaterial in $\{R < r < 2\}$ but has no lining on the interior surface of the metamaterial coating. In the limit $R \rightarrow 1^+$, solutions to Maxwell's equations have singular current terms K_{surf} and J_{surf} that represent either surface currents or the blow up of the D and B fields. A standard assumption in homogenization theory is that the length scale, d , of the substructures (or cells) from which a composite medium is formed, is much less than the free space wavelength λ of the EM field [30]. In treatments of homogenization for metamaterials, e.g., [31], it has been observed that effective material parameters can often be obtained even when d is not greatly less than λ . Although not explicitly stated, it is however required that sampled surface integrals of E, H, B , and D not vary greatly from point to point within a metamaterial cell. The blow up of B that we have shown occurs when cloaking without an SHS lining thus presents a challenge to the effective medium interpretation of the metamaterials employed.

(2) An infinite cylinder of air or vacuum is coated with metamaterial in $\{R < r < 2\}$ and equipped with an SHS-lining on the interior of the cloaking surface. The lining can be considered as parallel PEC and PMC strips, that allow surface currents in the z -directions. In this case, when $R \rightarrow 1^+$, the total E and H fields at the boundary have very small θ -components, that is, in the limit the tangential components of E and H are z -directional. The non-zero tangential boundary values of E and H correspond physically to surface currents, that are now allowed because of the SHS lining. Since the surface lining and fields are now compatible, the fields do not blow up. In addition, the amplitude of the far field pattern is greatly reduced.

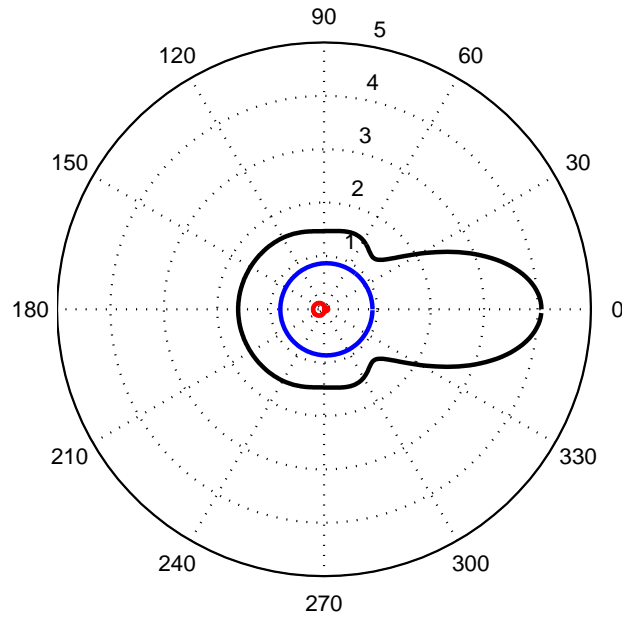


Fig. 5. **The magnitudes of the far field patterns of the scattered fields when $L_R = 1600$.** Black curve: far field pattern scattered from a perfectly conducting cylinder. Blue curve: Scattering from the invisibility coating without any physical lining. Red curve: Scattering from invisibility coated cylinder with a SHS lining.

Added in proof: See also the recent preprint [32], which studies approximate spherical cloaking for electrostatics, i.e., at $k = 0$., in dimensions two and higher.

Acknowledgements: A.G. was supported by NSF-DMS; M.L. by CoE-program 213476 of the Academy of Finland; and G.U. by NSF-DMS and a Walker Family Endowed Professorship.